



Published in final edited form as:

Pediatr Res. 2018 September ; 84(3): 435–441. doi:10.1038/s41390-018-0083-z.

Functional Characterization of Biallelic *RTTN* Variants Identified in an Infant with Microcephaly, Simplified Gyral Pattern, Pontocerebellar Hypoplasia, and Seizures

Jennifer A. Wambach¹, Daniel J. Wegner¹, Ping Yang¹, Marwan Shinawi¹, Dustin Baldrige¹, Ewelina Betleja², Joshua S. Shimony³, David Spencer⁴, Brian P. Hackett¹, Marisa V. Andrews¹, Thomas Ferkol¹, Susan K. Dutcher⁵, Moe R. Mahjoub², and F. Sessions Cole¹

¹Edward Mallinckrodt Department of Pediatrics, Washington University School of Medicine and St. Louis Children's Hospital, St. Louis, Missouri

²John T. Milliken Department of Medicine, Washington University School of Medicine and St. Louis Children's Hospital, St. Louis, Missouri

³Mallinckrodt Institute of Radiology, Washington University School of Medicine and St. Louis Children's Hospital, St. Louis, Missouri

⁴McDonnell Genome Institute, Washington University School of Medicine and St. Louis Children's Hospital, St. Louis, Missouri

⁵Department of Genetics, Washington University School of Medicine and St. Louis Children's Hospital, St. Louis, Missouri

Abstract

Background—Biallelic deleterious variants in *RTTN*, which encodes rotatin, are associated with primary microcephaly, polymicrogyria, seizures, intellectual disability, and primordial dwarfism in human infants.

Methods and Results—We performed exome sequencing of an infant with primary microcephaly, pontocerebellar hypoplasia, and intractable seizures and his healthy, unrelated parents. We cultured the infant's fibroblasts to determine primary ciliary phenotype.

Results—We identified biallelic variants in *RTTN* in the affected infant: a novel missense variant and a rare, intronic variant that results in aberrant transcript splicing. Cultured fibroblasts from the infant demonstrated reduced length and number of primary cilia.

Conclusion—Biallelic variants in *RTTN* cause primary microcephaly in infants. Functional characterization of primary cilia length and number can be used to determine pathogenicity of *RTTN* variants.

Users may view, print, copy, and download text and data-mine the content in such documents, for the purposes of academic research, subject always to the full Conditions of use:http://www.nature.com/authors/editorial_policies/license.html#terms

Corresponding Author: Jennifer A. Wambach, M.D., M.S., Campus Box 8116, 660 S. Euclid Ave, St. Louis, MO 63110, Phone: (314) 454-2683, Fax: (314) 454-4633, wambach_j@kids.wustl.edu.

Disclosure Statement: None of the authors has financial disclosures to report.

Introduction

Autosomal recessive primary microcephaly (MCPH) is a rare, heterogeneous neurodevelopmental disorder characterized by developmental disruption of brain growth including reduced cerebral cortex, simplified gyri, reduced white matter volume, abnormalities of the corpus callosum, and intellectual disability.(1, 2) At least 18 genes have been linked to MCPH,(3) with variants in *ASPM*(4) and *WDR62*(5) identified most frequently.(3, 6) Most of these genes encode components of basal bodies and centrosomes(7) illustrating the significant role of primary cilia in normal brain development.

RTTN encodes rotatin, a centrosome-associated protein that co-localizes to the basal bodies of primary cilia(8) and is required for appropriate expression of nodal, lefty2, and pitx2 in the left lateral plate mesoderm of the developing mouse embryo.(9) Mouse embryos lacking rotatin demonstrate abnormal heart looping, delayed neural tube closure, and alterations of left-right sidedness.(9, 10) Biallelic *RTTN* variants have been identified among infants and children with primary microcephaly, polymicrogyria, seizures, intellectual disability, and somatic growth impairment, (Table 1), (7, 8, 11) and fibroblasts from these individuals demonstrate shortened cilia.(8) We present a male infant with primary microcephaly, simplified gyri, pontocerebellar hypoplasia, contractures, and intractable epilepsy with a novel missense and a rare, intronic variant in *RTTN* that results in an aberrantly spliced transcript and reduced length and number of cilia in fibroblasts. Our data expand the genotypic and phenotypic spectrum for MCPH that results from genetic disruption of *RTTN* and demonstrate the usefulness of ciliary length and number for functional characterization of *RTTN* missense variants.

Methods

Clinical Report

A male infant of European-descent was born at 33 weeks gestation to a 38 year old primigravid mother whose pregnancy was complicated by the antenatal detection of calcifications of the fetal liver and cardiac intraventricular septum with non-diagnostic maternal serum *Toxoplasma gondii* and cytomegalovirus studies, shortening of the fetal long bones, polyhydramnios, pregnancy induced hypertension, pre-pregnancy maternal hyperthyroidism treated with thyroidectomy and thyroid hormone replacement, and preterm, premature rupture of membranes for which mother received antenatal corticosteroids and magnesium. The infant was delivered via caesarean section due to non-reassuring fetal surveillance. The infant required resuscitation at birth including intubation and mechanical ventilation. Family history was significant for a paternal grandfather with childhood seizures and a maternal grandfather with young-onset Parkinson's disease.

His birth measurements were: weight 1710g (−0.78 standard deviation (SD) below mean), length 38cm (−2.1 SD), and occipitofrontal circumference (OFC) 28cm (−1.5 SD). His measurements at 6 weeks of age were: weight 1950g (−3.4 SD), length 42.5cm (−3.4 SD), and OFC 27.5cm (−4.9 SD). Of note, OFC measurement at 6 weeks (27.5cm) was decreased from birth (28cm), possibly related to neonatal caput succedaneum or inter-individual differences in measurement. OFC measurement at 6 weeks was confirmed by a clinical

geneticist and a pediatric neurologist. Physical findings included relative microcephaly with metopic ridging, occipital prominence, bilateral microphthalmia, reactive pupils, microstomia, microretrognathia, smooth philtrum, relatively large, cupped, low-set ears, bilateral contractures of knees and ankles, mild camptodactyly with contractures of interphalangeal joints, bilateral syndactyly of fourth and fifth fingers and second to fifth toes, microphallus, cryptorchidism, and appendicular hypertonia with normal deep tendon reflexes.

Shortly after birth, the infant developed clinical seizures with head turning and extension of all extremities. His electroencephalogram demonstrated suppressed background and intermittent burst suppression that arose independently from both hemispheres. Despite aggressive anti-epileptic treatment with phenobarbital, fosphenytoin, levetiracetam, lorazepam, midazolam, pyridoxine, leucovorin, vigabatrin, and topiramate, his seizures persisted with multiple events per day. He died at 4 months of age after developing acute, progressive respiratory failure.

His diagnostic evaluation included magnetic resonance imaging of his brain that was notable for cerebral hypoplasia with simplified gyral pattern, pontocerebellar hypoplasia, bilateral frontal cortical dysplasia, agenesis of the corpus callosum, thinning of the periventricular white matter with *ex vacuo* dilatation of the occipital and temporal horns, misshapen orbital globes, and optic nerve hypoplasia (Figure 1). Ophthalmologic evaluation demonstrated rudimentary retinal vasculature, hypoplastic optic nerves, and pale optic disks. Skeletal radiographs demonstrated gracile appearing bones with thin ribs, hypoplastic mandible, increased density of the temporal bones, and soft tissue syndactyly. Renal ultrasound showed bilateral pyelocaliectasis. Cytomegalovirus and *Toxoplasma gondii* studies, serum amino acids, urine organic acids, lactate, pyruvate, thyroid studies, 7-dehydrocholesterol (7-DHC) reductase (to exclude Smith-Lemli Opitz syndrome), routine newborn screen, and chromosomal microarray analysis were non-diagnostic. Autopsy was not performed.

Exome sequencing

This study was approved by the Human Research Protection Office at Washington University. After parental informed consent was obtained, genomic DNA was isolated from the proband's skin fibroblasts and from parental saliva. Exome capture was performed using the Nimblegen VCRome v2.1 Exome kit (Roche, Madison, WI) with paired-end sequencing (2×125bp) on an Illumina HiSeq 2500 instrument (Illumina, San Diego, CA). Sequence reads were aligned to the human reference genome sequence (GRCh37/hg19) with 90% of the exome having at least 20x coverage. Variants were annotated with Annovar (<http://annovar.openbioinformatics.org/en/latest/>).⁽¹²⁾ Variants in coding regions and near exon-intron junctions that were novel or rare (minor allele frequency less than 0.01 in the Exome Aggregation Consortium (ExAC) database, (exac.broadinstitute.org))⁽¹³⁾ were assessed for predicted pathogenicity using Combined Annotation Dependent Depletion (CADD, cadd.gs.washington.edu),⁽¹⁴⁾ SIFT (sift.jcvi.org),⁽¹⁵⁾ Polyphen2 (genetics.bwh.harvard.edu/pph2/),⁽¹⁶⁾ LRT (genetics.wustl.edu/jflab/lrt_query.html),⁽¹⁷⁾ MutationTaster (www.mutationtaster.org),⁽¹⁸⁾ GERP++ (mendel.stanford.edu/SidowLab/downloads/gerp/),⁽¹⁹⁾ and PhyloP (<http://compugen.cshl.edu/phast/help-pages/phyloP.txt>).⁽²⁰⁾ Exonic variants

were classified as deleterious if predicted to be pathogenic by the majority of these programs. We used the dbSNV database(21) within Annovar to assess variants in splicing consensus regions. We evaluated for *de novo*, autosomal recessive, and X-linked recessive transmission, and candidate genes were reviewed for possible associations with the clinical phenotype.

Exon level oligo array comparative genomic hybridization (CGH) (ExonArrayDx) for the coding exons of the candidate gene was performed in a clinical laboratory (GeneDx, Gaithersburg, MD) on DNA obtained from the proband. Probe sequences and location were based on human genome build 19. Array CGH alterations were reported according to the International System for Human Cytogenetic Nomenclature (ISCN) guidelines.

Transcript Characterization

We extracted RNA from the proband's skin fibroblasts (RNeasy RNA extraction kit (Qiagen, Germantown, MD)) and from parental peripheral blood (PaxGene RNA tubes and blood RNA kit (Qiagen, Germantown, MD)) and synthesized cDNA using SuperScript III (Invitrogen, Carlsbad, CA). To assess RNA splicing, we designed PCR primers that would specifically amplify cDNA that includes exons 1 through 5, spanning several splice junctions. To test for possible aberrant splicing from a cryptic splice site in intron 1, we designed a primer pair in which the forward primer was located in intron 1, and the reverse primer in exon 3. To characterize RNA splicing further, we ligated Illumina adaptors to our PCR products, and performed deep resequencing on an Illumina Miseq instrument (Illumina, Carlsbad, CA).

To evaluate for aberrant splicing in a larger cohort, we queried the GTEx database (gtexportal.org) which contains 8,812 RNA-seq BAM files from 551 individuals for 55 tissue types to tabulate raw read counts for splice junctions. Briefly, data from each RNA-seq experiment were filtered to obtain spliced reads (containing the 'N' CIGAR operation) with mapping quality >20 that overlap the genomic interval of interest. Splice junctions were calculated from read mapping positions and the gapped alignment information contained with the CIGAR string. The number of reads supporting each unique junction was counted for each sample. Splice junctions were compared to Refseq gene annotations to define canonical versus non-canonical splicing events (e.g., exon skipping, alternate donor/acceptor sites, or alternate transcription start sites).

Ciliary Staining and Characterization

We cultured fibroblasts from the proband and a healthy control on coverslips maintained with 10% fetal bovine serum (FBS)/Dulbecco's minimal essential medium (DMEM). After fibroblasts reached 90% confluence, we arrested cell growth and facilitated ciliogenesis by reducing FBS/DMEM concentration (0.5%) for 48 hours. To assess cilia length and number, we performed immunofluorescent staining with anti- γ tubulin (to mark centrosomes) and anti-acetylated tubulin (to mark cilia). Briefly, after cell fixation with pre-chilled methanol (-20°C for 10 minutes) and washing with PBS and 0.1% Triton X-100 in PBS (PBS-T), cells were stained with monoclonal IgG1 anti- γ tubulin (1:1000, Sigma, St. Louis, MO) and monoclonal IgG2b anti-acetylated tubulin (1:10,000, Sigma, St. Louis, MO) for 1 hour.

After washing cells with PBS-T, cells were incubated with goat anti-mouse IgG1 Alexa Fluor 488 and goat anti-mouse IgG2b Alexa Fluor 594 (Invitrogen, Carlsbad, CA) for 1 hour. Images were captured with a Nikon Eclipse Ti-E inverted microscope and a wide-field immunofluorescence microscope. At least 100 cells were scored for the presence or absence of cilia. We used Chi square testing to compare the percentage of ciliated cells. We used Image J (<https://imagej.net>) to measure cilia length and Student's t-test to compare cilia length in the proband and control fibroblasts.

Magnetic Resonance Imaging Scanning

Images were collected on a Siemens Magnetom Trio 3T scanner. Structural images were collected with an axial magnetization-prepared rapid gradient-echo (MP-RAGE) T1-weighted sequence (time of repetition/echo time [TR/TE] 1550/3.05 ms and voxel size 1 mm³) and a turbo spin-echo T2-weighted sequence (TR/TE 8950/161 ms, voxel size 1 mm³, and echo train length 15).

Results

Exome Sequencing

We identified 2 rare variants in *RTTN* in the proband inherited in *trans*: a novel, predicted deleterious (CADD score=33)(14) missense variant, c.190G>T; p.Val64Phe, inherited from mother that is not present in the ExAC database [accessed May, 2018] and a rare, intronic variant (c.32-3C>T) inherited from father (frequency of 0.0073 in ExAC).(Supplemental Figure S1) Clinical exon level oligo array CGH did not detect any deletions or duplications that include the *RTTN* locus.

Transcript Characterization

We speculate that the c.32-3C>T variant results in leaky splicing (22) that concurrently produces canonical and aberrantly spliced (exon 2 skipping and activation of a cryptic splice site with partial intron 1 retention) cDNA transcripts. To assess exon 2 skipping, we designed primers to amplify the cDNA region from exon 1 to exon 5 of *RTTN* (primers listed in Supplement). Agarose gel electrophoresis (Supplemental Figure S2a) revealed an expected band size from the canonical transcript of 601 base pairs (bp) (Supplemental Figure S3a), but also a much lower abundance, smaller band at 407 bp in all samples. Gel extraction and Sanger sequencing of individual bands confirmed that the 601 bp band was the expected canonical transcript, and the 407 bp lower band lacked exon 2 (Supplemental Figure S3b). The identification of the exon 2 missense variant from the proband's 601 bp band indicates that some canonical splicing is occurring from both alleles. Since the sample from the mother, who is not a carrier of the c.32-3C>T splice variant, also showed a much lower abundance 407 bp band consistent with exon 2 skipping, we performed deep next generation sequencing on the PCR products to assess the relative amounts of canonical and aberrantly spliced alleles in each member of the family and in 4 unaffected control samples. We detected much more aberrantly spliced cDNA in the proband and father than in the mother and controls (Supplemental Table).

To assess the possibility of leaky activation of a cryptic splice site upstream in intron 1, we designed a primer pair in which the 5' (forward) primer was located in intron 1, and the 3' (reverse) primer was located in exon 3. PCR amplification of cDNA produced a band only in the samples from the subjects who carried the c.32-3C>T variant (proband and father) and not from the mother's sample (Supplemental Figure 2b). Gel extraction and Sanger sequencing of this amplicon revealed intron 1 sequence, but canonical exon2-exon3 splicing, suggesting this variant also results in retention of intron 1 (Supplemental Figure S3c). This finding indicates the c.32-3>T variant also results in an aberrantly spliced transcript from an upstream alternate splice site. However, the very small size of the exon 1-intron 1 region (~60 bp) precluded sufficient amplification and genomic resolution to confirm this additional aberrant transcript sequence.

As we detected some aberrant transcript in the samples from the mother and 3 controls and an alternate splice site in the samples from the proband and the father, we queried the GTex database to tabulate raw read counts for splice junctions involving exons 1–3 of *RTTN*. We found 146 (0.8%) reads in which exon 2 was skipped compared to 18,330 reads which demonstrated canonical exon 1-exon 2 splicing, demonstrating a low level of aberrant splicing in unrelated individuals. Of note, the canonical junction is supported by a mean of only 2 reads per sample in the GTex database, in contrast to our NextGen data with greater than 300x coverage per sample. In addition, the aberrantly spliced transcript is smaller than the canonical transcript (407 bp vs. 601 bp) and is likely to be preferentially amplified.

Immunofluorescent Staining

Biallelic variants in *RTTN* have been shown to cause defects in ciliary assembly.(8) We identified fewer ciliated cells (28% ciliated vs. 89% ciliated, $p < 0.0001$) and shorter cilia ($2.4 \pm 0.8 \mu\text{m}$ vs. $3.7 \pm 1.5 \mu\text{m}$, $p < 0.0001$) from the proband fibroblasts as compared to the control fibroblasts (Figure 2) in 3 independent experiments.

Discussion

Rotatin, a 2,226 amino acid protein, contains 2 highly conserved, armadillo-type fold domains that mediate protein-protein interaction.(8–10) Both the c.190G>T (p.Val64Phe) and the c.32-3C>T variants are located in the genomic region that encodes the first armadillo-type fold domain. Other variants (p.Cys27Tyr, p.Ala578Pro, p.His865Arg) within this region have been previously identified among individuals with microcephaly, abnormal gyri, and seizures(6–8) and suggest the importance of this domain for normal function and formation of primary cilia and for subsequent neurodevelopment. The *RTTN* variants identified among infants and children with primary microcephaly have been missense or splicing variants, suggesting that biallelic null variants may be embryonic lethal as described for another microcephalic primordial dwarfism gene *DONSON*.(23)

In silico splicing software predicts that the native 3' splice site near exon 2 of the *RTTN* gene is relatively weak, and that the c.32-3C>T variant further reduces the strength of this site (Alamut®). Our experimental results suggest that a very low rate of exon 2 aberrant splicing occurs in unrelated, healthy individuals, but the c.32-3C>T variant substantially increases the rate of aberrant splicing. Unlike the novel p.Val64Phe variant, the c.32-3 C>T

variant is present in 882 heterozygous individuals in ExAC including 4 homozygous individuals without available clinical phenotype information. We demonstrate that the c.32-3C>T variant reduces strength of the native splice site and results in leaky splicing(22) in which some canonically spliced product is produced. We speculate individuals homozygous for this variant produce sufficient canonical transcript for neurodevelopmental viability. However, when in *trans* with a deleterious variant, a single c.32-3C>T variant is insufficient to achieve a threshold of expression to permit normal neurodevelopment. Shortened ciliary length of our patient's fibroblasts has been previously identified among other patients with biallelic *RTTN* variants(8) and supports the pathogenicity of these *RTTN* variants. The decreased number of ciliated fibroblasts from our patient has not been previously observed among fibroblasts from patients with biallelic *RTTN* variants.

Murine embryos with genetically abrogated rotatin expression demonstrate randomized heart looping, delayed neural tube closure, and abnormalities of left-right sidedness.(9, 10) The lack of congenital heart disease or situs abnormalities in our patient and in previously reported MCPH patients with *RTTN* variants suggests species-specific differences in the role of *RTTN*, fetal lethality associated with *RTTN*-mediated cardiac abnormalities, genetic redundancy for *RTTN* encoded functions during human cardiac development, or differences in phenotypic consequences between complete null alleles (murine model) and biallelic missense/splice variants observed among the infants and children. Genetic disruption of *RTTN* and its *Drosophila* homolog *Ana3* expression in murine and fly models, respectively, demonstrates the importance of rotatin in brain development.(9, 24) *Ana3* also localizes to centrioles and basal bodies, and *Ana3*-deficient flies are severely uncoordinated and die soon after larval emergence, a phenotype similar to mutants of other centriolar and basal body structural proteins which result in defective cilia of type I neurons.(24)

The neurologic (microcephaly, simplified gyral pattern, agenesis of the corpus callosum, cortical dysplasia, reduced white matter, and contractures) and extra-central nervous system (bilateral cryptorchidism, microphallus, and renal pyelocaliectasis) findings in our patient are similar to previously reported patients with biallelic *RTTN* variants.(7, 8, 11) However, his ophthalmologic findings (misshapen orbital globes, optic nerve hypoplasia, rudimentary retinal vasculature, and pale optic disks) and skeletal findings (gracile appearing bones, thin ribs, hypoplastic mandible, increased density of the temporal bones and syndactyly) have not been previously reported.

In conclusion, our results support and extend the association of biallelic *RTTN* variants with severe primary microcephaly and emphasize the usefulness of functional characterization of primary cilia length and number for assessment of pathogenicity of *RTTN* variants. While some individuals with *RTTN*-related microcephaly have survived into adolescence or even early adulthood,(7, 8, 11) our patient had intractable epilepsy and died at 4 months of age. While earlier identification of a candidate gene to account for his phenotype would likely not have changed his anti-epileptic management or his disease course, genomic diagnosis permitted prediction of recurrence risk and prenatal or pre-implantation genetic diagnosis.

Supplementary Material

Refer to Web version on PubMed Central for supplementary material.

Acknowledgments

Statement of Financial Support: This work was supported by grants from the National Institutes of Health (K08 HL105891 (JAW), K12 HL120002 (FSC), R21/33 HL120760 (FSC)), R01 HL128370 (MRM), the Eunice Kennedy Shriver National Institute of Child Health & Human Development (U54 HD087011 (JSS), the Children's Discovery Institute (FSC, JAW, MRM), and the Saigh Foundation (FSC).

The authors thank the Exome Aggregation Consortium Database; a full list of contributing groups can be found at <http://exac.broadinstitute.org/about>. The authors thank the Genotype-Tissue Expression (GTEx) Project which was supported by the Common Fund of the Office of the Director of the National Institutes of Health, and by NCI, NHGRI, NHLBI, NIDA, NIMH, and NINDS. The data used for the analyses described in this manuscript were obtained from the GTEx Portal on 01/05/2018. Author contributions and conflicts of interest: Conception and design: JAW, DJW, MS, DB, FSC. Acquisition, analysis, or interpretation of data: JAW, DJW, PY, MS, DB, MVA, EB, JSS, DS, MRM, FSC. Drafting and revising the manuscript for important intellectual content: JAW, DJW, PY, MS, DB, EB, JSS, DS, BPH, MVA, TF, SD, MRM, FSC. All authors have approved the final version and agree to be accountable for all aspects of the work in ensuring that questions related to the accuracy or integrity of any part of the work are appropriately investigated and resolved. None of the authors has conflicts of interest to declare. All of the authors have seen and approved the submission and take full responsibility for the manuscript.

References

1. Mochida GH, Walsh CA. Molecular genetics of human microcephaly. *Curr Opin Neurol*. 2001; 14(2):151–6. [PubMed: 11262728]
2. Adachi Y, Poduri A, Kawaguch A, Yoon G, Salih MA, Yamashita F, et al. Congenital microcephaly with a simplified gyral pattern: associated findings and their significance. *AJNR Am J Neuroradiol*. 2011; 32(6):1123–9. [PubMed: 21454410]
3. Zaqout S, Morris-Rosendahl D, Kaindl AM. Autosomal Recessive Primary Microcephaly (MCPH): An Update. *Neuropediatrics*. 2017
4. Desir J, Cassart M, David P, Van Bogaert P, Abramowicz M. Primary microcephaly with ASPM mutation shows simplified cortical gyration with antero-posterior gradient pre- and post-natally. *Am J Med Genet A*. 2008; 146A(11):1439–43. [PubMed: 18452193]
5. Bhat V, Girimaji SC, Mohan G, Arvinda HR, Singhmar P, Duvvari MR, et al. Mutations in WDR62, encoding a centrosomal and nuclear protein, in Indian primary microcephaly families with cortical malformations. *Clin Genet*. 2011; 80(6):532–40. [PubMed: 21496009]
6. Rump P, Jazayeri O, van Dijk-Bos KK, Johansson LF, van Essen AJ, Verheij JB, et al. Whole-exome sequencing is a powerful approach for establishing the etiological diagnosis in patients with intellectual disability and microcephaly. *BMC Med Genomics*. 2016; 9:7. [PubMed: 26846091]
7. Shamseldin H, Alazami AM, Manning M, Hashem A, Caluseiu O, Tabarki B, et al. RTTN Mutations Cause Primary Microcephaly and Primordial Dwarfism in Humans. *Am J Hum Genet*. 2015; 97(6):862–8. [PubMed: 26608784]
8. Kheradmand Kia S, Verbeek E, Engelen E, Schot R, Poot RA, de Coo IF, et al. RTTN mutations link primary cilia function to organization of the human cerebral cortex. *Am J Hum Genet*. 2012; 91(3): 533–40. [PubMed: 22939636]
9. Faisst AM, Alvarez-Bolado G, Treichel D, Gruss P. Rotatin is a novel gene required for axial rotation and left-right specification in mouse embryos. *Mech Dev*. 2002; 113(1):15–28. [PubMed: 11900971]
10. Chatterjee B, Richards K, Bucan M, Lo C. Nt mutation causing laterality defects associated with deletion of rotatin. *Mamm Genome*. 2007; 18(5):310–5. [PubMed: 17551791]
11. Grandone A, Torella A, Santoro C, Giugliano T, Del Vecchio Blanco F, Mutarelli M, et al. Expanding the phenotype of RTTN variations: a new family with primary microcephaly, severe growth failure, brain malformations and dermatitis. *Clin Genet*. 2016; 90(5):445–50. [PubMed: 26940245]

12. Wang K, Li M, Hakonarson H. ANNOVAR: functional annotation of genetic variants from high-throughput sequencing data. *Nucleic Acids Res.* 2010; 38(16):e164. [PubMed: 20601685]
13. Lek M, Karczewski KJ, Minikel EV, Samocha KE, Banks E, Fennell T, et al. Analysis of protein-coding genetic variation in 60,706 humans. *Nature.* 2016; 536(7616):285–91. [PubMed: 27535533]
14. Kircher M, Witten DM, Jain P, O’Roak BJ, Cooper GM, Shendure J. A general framework for estimating the relative pathogenicity of human genetic variants. *Nat Genet.* 2014; 46(3):310–5. [PubMed: 24487276]
15. Ng PC, Henikoff S. Predicting deleterious amino acid substitutions. *Genome Res.* 2001; 11(5): 863–74. [PubMed: 11337480]
16. Adzhubei IA, Schmidt S, Peshkin L, Ramensky VE, Gerasimova A, Bork P, et al. A method and server for predicting damaging missense mutations. *Nat Methods.* 2010; 7(4):248–9. [PubMed: 20354512]
17. Chun S, Fay JC. Identification of deleterious mutations within three human genomes. *Genome Res.* 2009; 19(9):1553–61. [PubMed: 19602639]
18. Schwarz JM, Cooper DN, Schuelke M, Seelow D. MutationTaster2: mutation prediction for the deep-sequencing age. *Nat Methods.* 2014; 11(4):361–2. [PubMed: 24681721]
19. Davydov EV, Goode DL, Sirota M, Cooper GM, Sidow A, Batzoglou S. Identifying a high fraction of the human genome to be under selective constraint using GERP++ *PLoS Comput Biol.* 2010; 6(12):e1001025. [PubMed: 21152010]
20. Cooper GM, Stone EA, Asimenos G, Program NCS, Green ED, Batzoglou S, et al. Distribution and intensity of constraint in mammalian genomic sequence. *Genome Res.* 2005; 15(7):901–13. [PubMed: 15965027]
21. Liu X, Wu C, Li C, Boerwinkle E. dbNSFP v3.0: A One-Stop Database of Functional Predictions and Annotations for Human Nonsynonymous and Splice-Site SNVs. *Hum Mutat.* 2016; 37(3): 235–41. [PubMed: 26555599]
22. Rogan PK, Faux BM, Schneider TD. Information analysis of human splice site mutations. *Hum Mutat.* 1998; 12(3):153–71. [PubMed: 9711873]
23. Reynolds JJ, Bicknell LS, Carroll P, Higgs MR, Shaheen R, Murray JE, et al. Mutations in DONSON disrupt replication fork stability and cause microcephalic dwarfism. *Nat Genet.* 2017; 49(4):537–49. [PubMed: 28191891]
24. Stevens NR, Dobbelaere J, Wainman A, Gergely F, Raff JW. Ana3 is a conserved protein required for the structural integrity of centrioles and basal bodies. *J Cell Biol.* 2009; 187(3):355–63. [PubMed: 19948479]

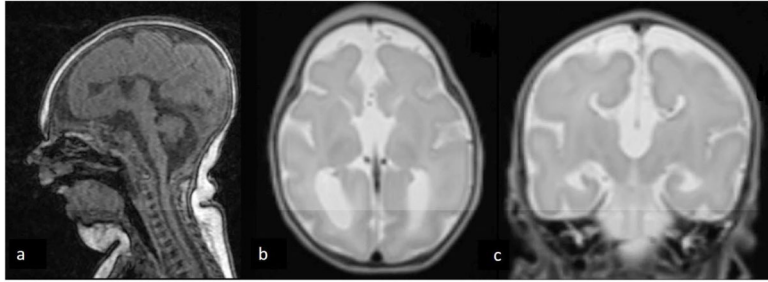


Figure 1abc.

MRI findings at term equivalent age. T1-weighted sagittal view (a) demonstrates cerebellopontine hypoplasia and micrognathia. T2-weighted transverse view (b) demonstrates enlarged occipital horns and agenesis of the corpus callosum with large third ventricle. T2-weighted coronal view (c) demonstrates typical ventricular configuration for agenesis of the corpus callosum with superior extension of an enlarged third ventricle. All three views demonstrate microcephaly and markedly delayed folding pattern for age.

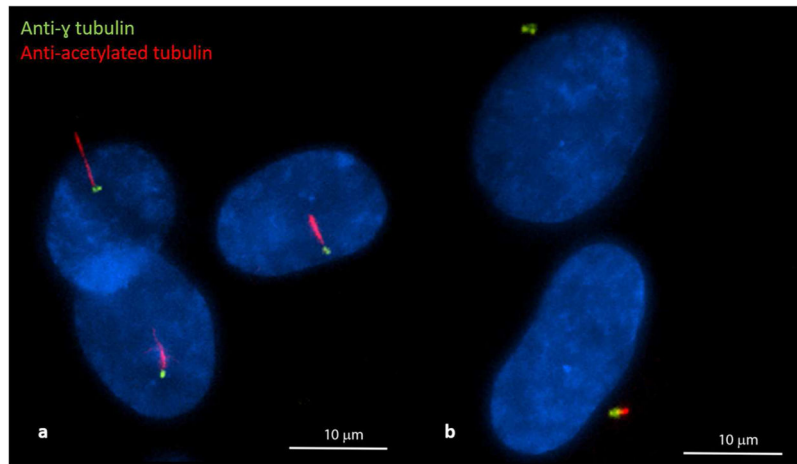


Figure 2. Comparison of confocal immunofluorescence microscopy images of control (a) and proband fibroblasts (b) demonstrate fewer ciliated cells and shortened cilia in the proband fibroblasts. Green fluorescent-labelled anti-gamma tubulin was used to stain centrosomes, red fluorescent-labelled anti-acetylated tubulin was used to stain primary cilia, and DAPI was used to stain nuclei.

Table 1

Clinical Findings of Proband (Subject 1) and Other Subjects with Recessive *R77N* Variants

		Previously Reported Patients									
Subject (S)	S1 (Proband)	S2	S3	S4	S5	S6	S7	S8			
Age #	Deceased 4 months	12 years	14 years	18 years	16 years	12 years	11 years	6 years			
Sex	Male	Male	Male	Female	Male	Male	Male	Male			
Family History	Negative	Affected brother (S3) and sister (S4)	Affected brother (S2) and sister (S4)	2 affected brothers (S2, S3)	Negative	2 affected brothers (S7, S8)	2 affected brothers (S6, S8)	2 affected brothers (S6, S7)			
Pregnancy/delivery	33 weeks	38 weeks	NR	NR	40 weeks	Term	NR	NR			
Head circumference (SD)	Age 6 weeks: 27.5cm	Age 12 years: -2.5 SD	Age 24 years: -2 SD	NR	Age 16 years: 0 SD	Age 12 years: 34.2cm (-8.2 SD)	Age 10 years: 34.4cm (-8.2 SD)	Age 6 years: 34.5cm (-8.2 SD)			
Height (SD)	Birth weight 1710g (-0.78 SD)	Age 12 years: -2 SD	Age 24 years: -1 SD	NR	Age 16 years: -2.5 SD	Age 12 years: 111cm (-5.6 SD)	Age 10 years: 95.5cm (-7.2 SD)	Age 6 years: 91.3cm (-5 SD)			
Weight (SD)	Birth weight 1710g (-0.78 SD)	Birth weight -2 SD	NR	NR	Birth weight: 0 SD	Birth weight: 1kg (-4.1 SD)	Age 10 years: 10.8kg (-12.6 SD)	Age 6 years: 9kg (-10.2 SD)			
Brain MRI Findings	Simplified gyri, ponto-cerebellar hypoplasia, intractable epilepsy	Asymmetric (R>L), irregular gyral pattern in posterior horns, white matter beneath cortical malformation, mildly enlarged lateral ventricles, thin corpus callosum	Extensive asymmetric (R>L), irregular gyral pattern in posterior horns, white matter beneath cortical malformation, mildly enlarged lateral ventricles, thin corpus callosum, small cerebellar vermis and hemispheres, mildly enlarged fourth ventricle	NR	Bilateral polymicrogyric cortex in temporal areas with associated white matter thinning, reduced parietal and occipital white matter, thin splenium of corpus callosum	Severe microcephaly, few sulci, shallow Sylvian fissures	NR	NR	NR	NR	
Other clinical features	Bilateral microphthalmia, microstomia, micrognathia, scooped palatum, bilateral contractures of knees and ankles, mild camptodactyly with contractures of inter-phalangeal joints, bilateral syndactyly of fourth and fifth fingers and second to fifth toes, bilateral hypotonia, appendicular hypotonia	Seizures, severe intellectual disability, small kidney volume	Seizures, moderate intellectual disability	Seizures, moderate intellectual disability	Seizures, severe intellectual disability	Single kidney, microcephaly related craniofacial dysmorphism, mild bilateral hypoplasia of kidneys, severe intellectual disability	NR	NR	NR	NR	
<i>R77N</i> variants	c.190G>T (p.Val64Phe) c.32>C>T	c.2796A>T (p.Leu932Phe) c.2796A>T (p.Leu932Phe)	c.2796A>T (p.Leu932Phe) c.2796A>T (p.Leu932Phe)	c.2796A>T (p.Leu932Phe) c.2796A>T (p.Leu932Phe)	c.803>A (p.Cys27Tyr) c.806>A (p.Cys27Tyr)	c.2885>A>G c.2885>A>G	c.2885>A>G c.2885>A>G	c.2885>A>G c.2885>A>G	c.2885>A>G c.2885>A>G	c.2885>A>G c.2885>A>G	
Reference		Kheradmand /	Kheradmand /	Kheradmand /	Kheradmand /	Shamseldin /	Shamseldin /	Shamseldin /	Shamseldin /	Shamseldin /	

		Previously Reported Patients									
Subject (S)	S9	S10	S11	S12	S13	S14	S15				
Age #	5.5 years	Newborn	Newborn	35 months	21 months	5 years	10 years				
Sex	Male	Male	Male	Male	Female	Female	Female				
Family History	Two healthy female siblings	Affected brother (S11)	Affected brother (S10)	Affected sister (S13)	Affected brother (S12)	Affected sister (S15)	Affected sister (S14)				
Pregnancy/delivery	34 weeks, severe IUGR	Term, severe IUGR	37 weeks	Term	Term	NR	NR				
Head circumference (SD)	Birth OFC: 26cm (-4.7 SD) Age 3 years: 34.5cm (-9.2 SD) Age 5.5 years: 36cm (-11.3 SD)	Birth OFC: 24cm (-5SD)	Birth OFC 24cm (-4.5SD)	Birth OFC: 28 cm (-5.3 SD) Age 35 mos: 34.8cm (-9.3 SD)	Birth OFC: 27 cm (-5.3 SD) Age 21 mos: 32cm (-10.5 SD)	-4.4 SD	-5.2 SD				
Height (SD)	Birth length: 38cm (-3.5 SD) Age 3 years: 75.2cm (-5.4 SD) Age 5.5 years: 92.1cm (-4.1 SD)	Birth Length: 31.5cm (-5 SD)	Birth length 34.5cm (-6 SD)	Birth length: 47cm (-2.3 SD) Age 35 mos: 75.5cm (-4.8 SD)	Birth length: 44cm (-2.9 SD) Age 21 mos: 63.6cm (-6.4 SD)	NR	NR				
Weight (SD)	Birth weight: 1590g (-2 SD) Age 3 years: 9kg (-3.9 SD) Age 5.5 years: 13.6kg (-2.8 SD)	Birth weight 1150g (-4 SD)	Birth weight 666g (-6 SD)	Birth weight 3kg (-1.47 SD) Age 35 mos: 7.5kg (-5.4 SD)	Birth weight 2.6kg (-1.7 SD) Age 21 mos: 6kg (-5 SD)	NR	NR				
Brain MRI Findings	Severe microcephaly with simplified gyration	Severe microcephaly, severe cerebellar and cerebellar hemispheres, dysgenesis of corpus callosum, large posterior cyst, multiple areas of lissencephaly and/or pachygyria and polymicrogyria, multiple subependymal gray matter heterotopias	Severe microcephaly, severe cerebellar and cerebellar sulcation, deformed ventricles, large CSF intensity areas occupying majority of supratentorial compartments bilaterally	Lissencephaly of frontal lobes, periventricular gray matter heterotopia, multiple areas of dysplasia, enlarged into right occipital region, pons hypoplasia	Lissencephaly, periventricular gray matter heterotopia, quadrate lobes, enlarged into right occipital region, pons hypoplasia	Diffuse pachygyria	Mild frontal lissencephaly, posterior frontal pachygyria, paraventricular heterotopia				

		Previously Reported Patients			
Other clinical features		Slowing forehead, high broad nasal bridge, multiple joint contractures, failure to thrive, death at 2 months from cardiopulmonary arrest	Slowing forehead, joint contractures, cryptorchidism, duodenal atresia, death at 17 days	Congenital dermatitis (diffuse eczema), receding forehead and chin, protruding nose, hypotelorism with prominent eyes, slightly upturned palpebral fissures, simple cleft lip, mild facial dysmaturity and speech delays	Congenital dermatitis (diffuse eczema), receding forehead and chin, protruding nose, hypotelorism with prominent eyes, slightly upturned palpebral fissures, simple cleft lip, mild facial dysmaturity and speech delays, motor and speech delays
RTTN variants	c.3190A>C (p.Lys1064Gln)(c.3190A>C (p.Lys1064Gln)	e.1732G>C (p.Ala578Pro)(c.5750A>G (p.Asp1917Gly)	e.1732G>C (p.Ala578Pro)(c.5750A>C (p.Asp1917Gly)	e.2953A>G (p.Arg985Gly)(c.2953A>C (p.Arg985Gly)	e.2953A>G (p.Arg985Gly)(c.2953A>G (p.Arg985Gly)
Reference	Shamseldin ²	Shamseldin ²	Shamseldin ²	Grandone ³	Rump ⁴

IUGR: intrauterine growth restriction; BW: birthweight; SD: standard deviation; OFC: occipitofrontal circumference; CSF: Cerebrospinal fluids; NR: not reported

* Age at time of observation

¹ Kheradmand Kia S, Verbeek E, Engelen E, Schot R, Poot RA, de Coo IF, Lequin MH, Poulton CJ, Pourfarzad F, Grosveld FG, Brehm A, de Wit MC, Oegema R, Dobyns WB, Verheijen FW, Mancini GM. RTTN mutations link primary cilia function to organization of the human cerebral cortex. *Am J Hum Genet.* 2012;91:533–40.

² Shamseldin H, Alazami AM, Manning M, Hashem A, Caluseiu O, Tabarki B, Esplin E, Schellei S, Innes AM, Parboosingh JS, Lamont R, Care4Rare Canada C, Majewski J, Bernier FP, Alkuraya FS. RTTN Mutations Cause Primary Microcephaly and Primordial Dwarfism in Humans. *Am J Hum Genet.* 2015;97:862–8.

³ Grandone A, Torella A, Santoro C, Giugliano T, Del Vecchio Bianco F, Mutarelli M, Cirillo M, Cirillo G, Piluso G, Capristo C, Festa A, Marzuillo P, Miraglia Del Giudice E, Perrone L, Nigro V. Expanding the phenotype of RTTN variations: a new family with primary microcephaly, severe growth failure, brain malformations and dermatitis. *Clin Genet.* 2016;90:445–50.

⁴ Rump P, Jazayeri O, van Dijk-Bos KK, Johansson LF, van Essen AJ, Verheij JB, Veenstra-Knol HE, Redeker EJ, Mannens MM, Swertz MA, Alizadeh BZ, van Ravenswaaij-Arts CM, Simke RJ, Sikkema-Raddatz B. Whole-exome sequencing is a powerful approach for establishing the etiological diagnosis in patients with intellectual disability and microcephaly. *BMC Med Genomics.* 2016;9:7.